Optimization of Combined Thermal and Electrical Behavior of Power Converters Using Multi-Objective Genetic Algorithms

Optimization of Combined Thermal and Electrical Behavior of Power Converters Using Multi-Objective Genetic Algorithms

D.V. Malyna, J.L. Duarte, M.A.M. Hendrix, F.B.M. van Horck
Technical University of Eindhoven
Electromechanics and Power Electronics Group, Den Dolech 2
5600MB Eindhoven, The Netherlands
Phone: +31 (0) 40 247-3568
Fax: +31 (0) 40 243-4364
Email: D.V.Malyna@tue.nl
URL: http://w3.ele.tue.nl/nl/evt/epe/

Acknowledgments

The authors would like to thank SenterNovem for their financial support under project code IOP-EMVT 02207 and Philips Power Solutions for the test samples and materials.

Keywords

<<Estimation technique>>, <<Modeling>>, <<Simulation>>, <<Thermal design>>

Abstract

A practical example of power electronic converter synthesis is presented, where a multi-objective genetic algorithm, namely Non-Dominated Sorting Genetic Algorithm (NSGA-II) is used. The optimization algorithm takes an experimentally-derived thermal model for the converter into account. Experimental results are provided for verification.

Introduction

Converter synthesis is a non-trivial problem which is not often addressed. A "trial and error" approach is a common technique in use today. Computer aided analysis software is capable of speeding-up the process of doing the trial runs and analyzing the errors. However, up to the present time synthesis must be manually performed by a designer, who selects a specific topology and determines the values of the converter parameters to obtain the required performance.

This paper presents a computer-oriented way of tuning converter parameters by using the custom software tool **M_SIM**. The tool is developed in the MATLAB environment as a set of interactive scripts for modeling and optimizing a power converter. **M_SIM** models power converters as piecewise-linear systems and simulates them by means of an accelerated algorithm for steady-state determination [4]. Thermal and electrical behavior are coupled together with an experimentally-extracted thermal model [5] and rules for the mutual thermal-electrical dependencies [5, 7]. **M_SIM** is capable of performing multi-objective optimization using the NSGA-II genetic algorithm [1].

The flowchart of design optimization is shown in Figure 1. The optimization assignment is input together with the converter circuit, the latter described by a netlist and a thermal model. An initial population of design variables is randomly generated and sequentially explored. For each set of the variables the converter is simulated by the accelerated algorithm to determine the electrical steady-state. After the electrical steady state is found, the temperatures are calculated by means of the provided thermal model. Iteration (see Figure 1) is used because the temperatures are influenced by the electrical losses, and the losses, in their turn, are influenced by the temperatures. In this way after a few iterations the converter is completely characterized. If a constraint violation occurs during this iteration, the fitness of that possible solution is downgraded. When all the members of the population are explored, genetic operations -

selection, crossover and mutation - are performed on the population. The abovementioned process is repeated for a pre-specified number of times, called the number of runs of the genetic algorithm.

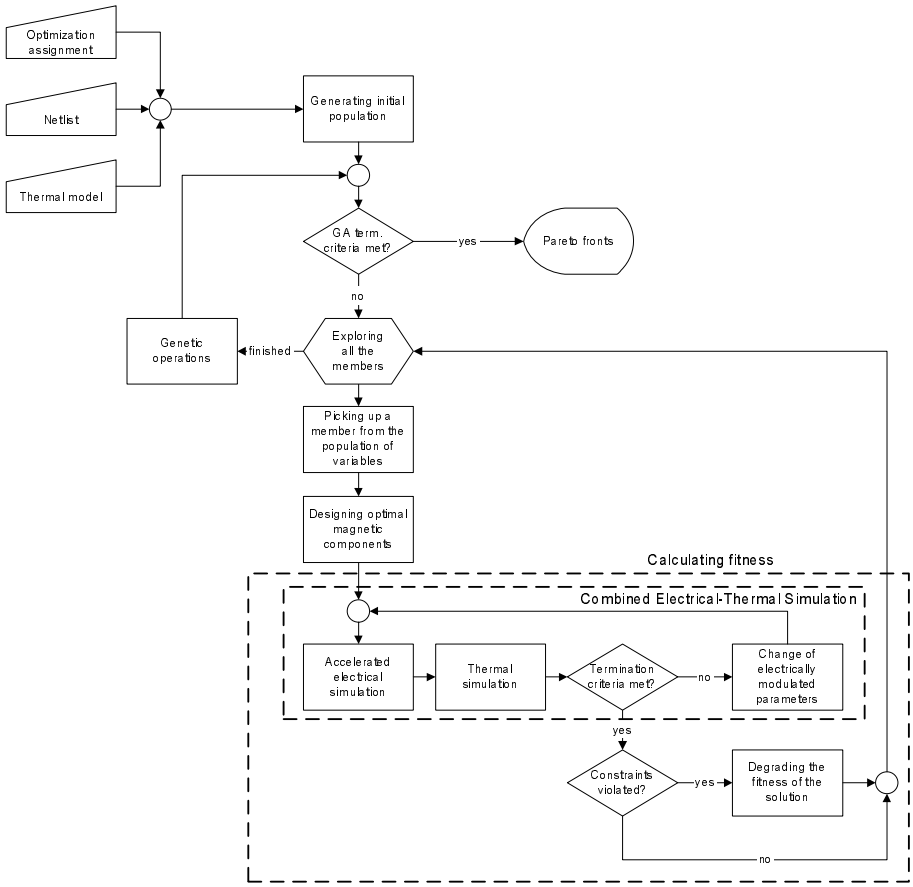

Figure 1: Converter optimization flowchart

Practical example

A commercial power supply was chosen as a test prototype (see Figure 2a). It contains several converters, but only the LLC (see Figure 2b) was modelled. The LLC's 24V output was loaded with a maximum current of 4.25A; the converter switches at the frequencies about 100kHz. The sources of heat dissipation (MOSFETs T1, T2, diodes D1, D2 and transformer Tr) are shown in Figure 2a with arrows. The winding and core losses of the transformer are taken into account.

Optimization assignment

When optimization of a power converter is performed, often the minimization of a converter volume is considered as the objective. Decreasing of this volume is even more restricted by heat dissipating capabilities of the components mounted on the PCB. The volume of the power converter is determined in first approximation by heatsinks, magnetic components and elcaps. However, the volume of magnetic component is mainly determined by a core type. The core type, is selected using the flux density and the criterion of fitting the windings to the window. The heat dissipative capabilities of the magnetic component are not utilized completely. Therefore, finding the trade-off between the power dissipated in the components mounted on the heatsinks and in the volumetric components, like transformers and inductors looks reasonable. The designer can find a balance between the losses in the magnetic component and the transistors, diodes, etc. mounted on the heatsink. The LLC converter of Figure 2 was used as the testbench to illustrate this approach.

The losses in the transistors and the diodes should be minimal in order to keep the heatsink sizes small, while the losses in the transformer can be increased if the temperature of the transformer stays within the reasonable range (below $90°C$).

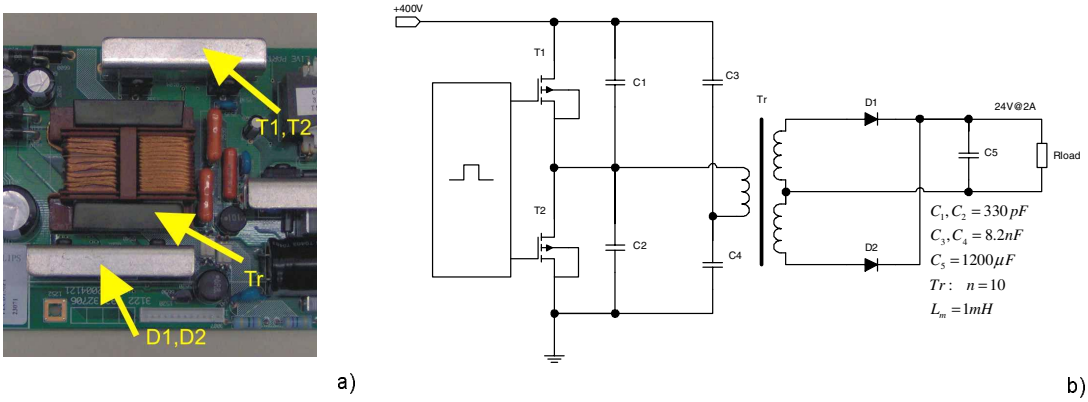

Figure 2: LLC converter : a) Photograph b) Schematic diagram

The values of the magnetizing inductance L_m of the transformer Tr, resonant capacitors $C3, C4$ and turns ratio n are used as design parameters (see Figure 2). The parameters are varied within a certain range in order to obtain desirable converter performance. The RMS value of the primary current of the transformer is chosen as one objective, because the losses in the transistors of the LLC are determined by the primary current, while the losses in the diodes of the output rectifier are determined mainly by the load current.

The input and output voltages of the LLC are specified, and, at the same time, the converter should maintain an acceptable level of the output ripple. Switching frequency of the LLC is changed within a certain range to control the transferred power. The optimization assignment is constrained by the ZVS of transistors $T1, T2$. In formal language, the optimization assignment for the LLC is formulated as

$$\begin{cases} min & (\Delta T_{core},\ i_{Trpri}(RMS)) \\ & L_m \in [500\,\mu H \ldots 1500\,\mu H] \\ & (C3+C4) \in [10\,nF \ldots 30\,nF] \\ & n \in [8 \ldots 12] \\ & u_{C5}(AVG) = 24\,V \\ & u_{C5}(\Delta) \leq 0.5\,V \\ & f \in [40\,kHz \ldots 200\,kHz] \\ & ZVS\ T1, T2 \\ & Opt.\ transformer \end{cases}, \tag{1}$$

where ΔT_{core} is a temperature increase of the transformer core over the ambient temperature, $i_{Trpri}(RMS)$ denotes the RMS value of the primary current of the transformer, $u_{C5}(AVG)$, $u_{C5}(\Delta)$ are the average value of output voltage and the output ripple voltage respectively, and f is a switching frequency.

Optimization of transformer

The function of optimizing transformers is included in **M_SIM**. The tool assumes that the transformer geometry, i.e. core type and coilformer, are fixed. In other words, only the winding of the transformer should be designed. This means choosing the proper wire and the number of turns in order to heat up the core to the maximum possible temperature. At the same time the temperature should be the highest within the allowed operating range. It is logical to suppose that the component, which is utilized in the best way, has the highest temperature [1]. The temperature of the transformer is determined by the core losses and the winding losses. The core losses depend on the flux density in the core and the switching frequency, while the winding losses depend on the resistance of the winding and the current that flows through the winding [12]. Therefore, flux density B is considered as the primary design parameter that is varied within a certain range to obtain the highest temperature of the transformer. Magnetizing inductance L_m and turns ratio between primary and secondary windings n are the parameters that are defined by the optimized power converter circuit. The maximum allowed temperature T_{lim}, maximum allowed dissipation P_{lim}, saturation flux density B_{sat}, and width of the transformer window h_{window} restrict the feasible transformer designs. The restriction on the losses is determined by the efficiency of the

[1] However, at this point it is important to recognize that high temperatures caused by a poor design are out of scope of this research

converter, while the transformer window size determines the maximum allowed width of the windings in order to fit the windings to the transformer window. In formal language, the transformer optimization assignment is expressed as

$$\begin{cases} Find & max(\Delta T) = f(B) & & \\ Given & L_m, n & & \\ & B & < & B_{sat} \\ & (\Delta T + T_{amb}) & < & T_{lim} \\ & (P_{core} + P_{winding}) & < & P_{lim} \\ & h_{winding} & < & h_{window} \end{cases}, \tag{2}$$

where ΔT is the transformer's temperature increase over the ambient temperature T_{amb}, P_{core} and $P_{winding}$ are the losses in the core and in the windings respectively, $h_{winding}$ is the width of the winding.

Determination of the design parameters like flux density, the losses in the core and in the winding, require the currents and the switching frequency of the power converter. But those parameters are not known to **M_SIM** in advance. Therefore the converter is simulated with an ideal transformer to determine the winding currents and the switching frequency. The magnetizing current is obtained as the superposition of the currents of the primary and the secondary windings. The optimal transformer is designed afterwards according to (2). After the transformer is completely characterized, the winding resistances and the equivalent core loss resistance are inserted into the netlist. The combined electrical-thermal simulation is then performed as described in [7].

Temperature ΔT of the transformer is expressed as a function of flux density B using the method [8]. The number of turns and the airgap are determined first. Secondly the winding is designed using the required wires (see Table I). Therefore, the number of layers, the number of turns per layer, winding width, etc. are determined and electrical parameters of the windings, i.e. the DC resistances and the AC resistances at the specified switching frequency are determined. At the same time, the windings are checked to fit the window. Finally, electrical losses and the cost of the wire are calculated, because **M_SIM** considers the trade-off between winding losses and the wire cost to obtain the optimal winding design. In such a way the best winding is chosen and next the leakage inductance and the coupling coefficient are determined for calculating the parameters of the coupled inductors model [14]. Finally, the estimates of the core losses and the temperature of the transformer are obtained; the constraints are checked afterwards. The termination criterion of achieving the maximum ΔT is checked and the next iteration of the transformer optimization loop is performed, or, alternatively, the transformer is considered to be designed, and **M_SIM** simulates the converter with the non-ideal transformer.

Table I: Parameters of transformer optimization related to (2)

Core type	Ferrite	Windings	B_{sat}	T_{amb}	T_{lim}	P_{lim}
U-type	3C94	10x0.1, 30x0.1, 60x0.1 6x0.2, 10x0.2, 15x0.2	0.3 T	333 K ($60^{\circ}C$)	363 K ($90^{\circ}C$)	3.5 W

Thermal model

The thermal model of the LLC was derived experimentally using the method described in [5]. Consider that heat-dissipative components $\{1 \dots n\}$ are located on the PCB and electrical dissipation (power $\mathbf{P} = \{P_1 \dots P_n\}$) is injected into each of them (see Figure 3). The resulting temperature increase of each component $\Delta\mathbf{T} = \{\Delta T_1 \dots \Delta T_n\}$ is measured and registered together with the injected losses $\mathbf{P}$. The experiment is performed several times with different values of $\{P_1, \dots, P_n\}$ to collect the necessary data for identification of matrix $\mathbf{R_\theta}$ in (4).

A linearized thermal model is assumed as

$$\Delta\mathbf{T} = \mathbf{R}_\theta(\mathbf{P} - \mathbf{P}_0) + \Delta\mathbf{T_0}, \tag{3}$$

where $\mathbf{P}$ is a vector whose entries are the actual losses, $\mathbf{P}_0$ are losses at a particular operating set point, $\Delta\mathbf{T_0}$ is the initial temperature offset (above ambient temperature) corresponding to $\mathbf{P}_0$, $\Delta\mathbf{T}$ is the resulting temperature offset (above ambient temperature) corresponding to $\mathbf{P}$, and $\mathbf{R_\theta}$ is the matrix of thermal resistances.

The extraction procedure for the model was improved with respect to [5]. A modified setup for extraction of the thermal model was built (see Figure 4). The measured board is placed inside a closed chamber

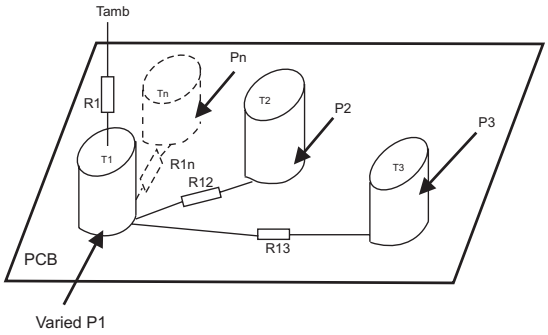

Figure 3: Experimental method for deriving the thermal model

which is capable of controlling the temperature to 0.1 degree, and supplies a stable airflow during the entire run of the experiment (30 minutes per measured point). The model is identified with a verified maximum error of 10% using the least-squares method of [13].

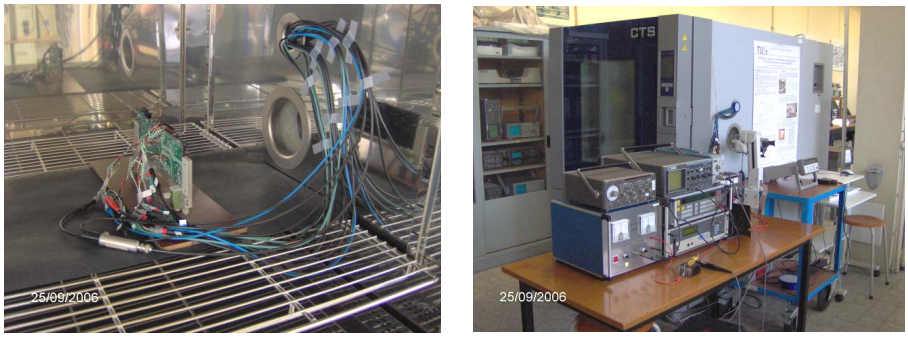

a) b)

Figure 4: A setup for experimental identification of the thermal model: a) General view of the setup b) Converter under investigation

Optimization results

At the present time, NSGA-II is reported to be one of the most efficient multi-objective optimization algorithms [9], and, therefore, the assignment of optimization is solved by applying NSGA-II as suggested by [6]. The number of points and chromosome length are determined as $N_{memb} = 10$, and $N_{gen} = 12$ respectively to achieve the highest processing rate of the genes [2]. The algorithm was executed for the specified number of runs $N_{runs} = 50$, as suggested in [10], and produced the Pareto front as shown in Figure 5b and listed in Table II.

The quality of the optimization will be evaluated by the brute-force simulation over all the points in the search variable space. Since the search variables are represented by a 4-bit chromosome, the resulting number of points per each objective is $2^4 = 16$, and $16^3 = 4096$ possible combinations for the three variables. As it follows from Figure 5a the span of the objective is quite large. However, only the points 1–17 satisfy the criterion of optimality (1). The optimal points, that are discovered by brute-force are presented in Figure 5b together with the results of GA optimization. The GA method discovered two points of the original Pareto front, the points 3 and 6. The extreme points of the Pareto front, the points 1 and 17, were also approached very closely by the GA. The maximum deviation of the points produced by the GA from the real Pareto front is about 10 mA and 2 K for the point 1 of the GA method and point 2 of the brute-force.

It is important to recognize that GA is a stochastic optimization algorithm, and it is capable of only approaching the front. In other words, it is meaningless to expect to find exact values with absolute certainty because of stochastic nature of the algorithm.

The tool designs for every point of Figure 5 another optimal transformer. Actually, a more fundamental approach would include the parameters of transformer, like the number of turns, airgap, the type of

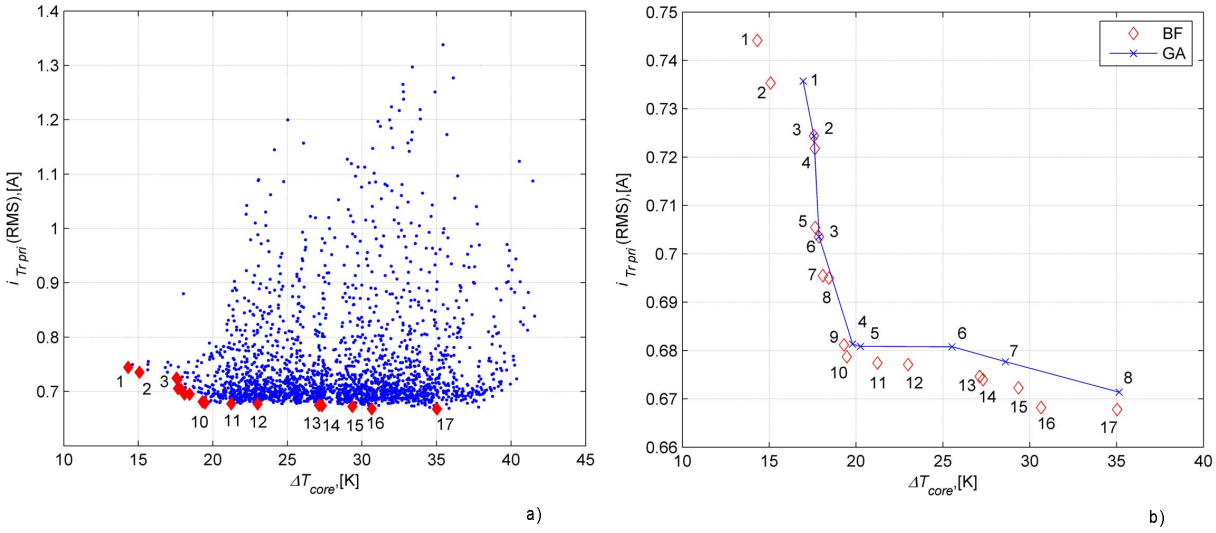

Figure 5: Pareto fronts of: a) Brute-Force search b) GA optimization and brute-force (BF) search

Table II: The optimal converter designs of Figure 5

Point	Variable			Objective function		Switching frequency
	L_m $[\mu H]$	$C3+C4$ $[nF]$	n	ΔT_{W1} $[K]$	$i_{W1pri}(RMS)$ $[A]$	f $[kHz]$
1	567	19.33	9.87	16.95	0.736	148.0
2	567	28.67	9.07	17.57	0.724	141.7
3	633	16.67	10.13	17.87	0.704	130.6
4	1167	27.33	10.13	19.79	0.681	69.9
5	1033	26.00	10.67	20.25	0.681	67.5
6	1300	15.33	12.00	25.53	0.681	54.8
7	1233	18.00	11.73	28.60	0.678	51.8
8	1100	11.33	11.73	35.14	0.671	63.1

the wire, the flux density etc. as the parameters of the GA. The only drawback is that the number of parameters is too large to be verified by the brute-force method. The number of brute-force evaluations is determined as $\left(2^{N_{var}} \cdot N_{gen}\right)$ and in the particular case of $N_{var} = 3$, $N_{gen} = 4$ is 4096 points, resulting in approximately 9-day simulation. In the case of $N_{var} = 6$, $N_{gen} = 4$ the number of points is 16777216 and that results in 20480 days or 56-year simulation. Therefore, the assignment of optimization is split by two subparts - optimization of the transformer and optimization of the converter with the optimal transformer.

Verification of the results

The results of the optimization were verified by taking two points of the Pareto front, point 3 (where the results of both methods coincided) and point 7 (the point on the right-hand side of the front). The optimal transformers were verified by building them with the specified wire and the number of turns (see Table III).

The corresponding primary and secondary number of turns were wound first with the specified wire. The DC and AC resistances at the frequencies that are specified in Table III were measured and registered in Table IV. Next, the core airgap was adjusted by measuring primary inductance L_p at the corresponding frequency with the impedance analyzer while the terminals of secondary winding were left open. After the primary inductance is adjusted, the half-cores are tightened and glued together. The measurement of secondary inductance with open primary terminals and mutual inductance between the primary and the secondary was performed using the method of [3]. Coupling coefficient k between primary and secondary

Table III: Data of the optimal transformers

Parameter name	Notation	Value
Transformer of point 3 (see Table II)		
Number of primary turns	n_{turns}	36
Number of secondary turns	$n_{turns}(sec.)$	4
Wire	–	0.2x10
Airgap	ℓ_{gap}	0.23 mm
Primary inductance	L_p	675 μH
Design frequency	f	97.3 kHz
Transformer of point 7 (see Table II)		
Number of primary turns	n_{turns}	48
Number of secondary turns	$n_{turns}(sec.)$	4
Wire	–	0.2x10
Airgap	ℓ_{gap}	0.21 mm
Primary inductance	L_p	1279 μH
Design frequency	f	55.1 kHz

windings was calculated [14] and compared with the targeted value (see Table IV). The targeted and the realized values are compared by calculating the discrepancies as

$$\delta_{Param} = \frac{|Param_{realized} - Param_{targeted}|}{Param_{realized}} \times 100\%, \tag{4}$$

where $Param_{realized}$ and $Param_{targeted}$ are realized and targeted values of the parameter respectively. The discrepancy between the realized and targeted parameters of the transformers is within the range of 10% – 15%.

During optimization of the LLC the values of resonant tank capacitors C3 and C4 are varied. The obtained value of capacitance (see Table IV) was implemented using film capacitors. Since physical components are used, the manufacturing tolerances should be considered. The capacitances were measured with the impedance analyzer and listed in Table IV. For design #3 the discrepancy is 3.3% and for design #7 it equals only 0.5%.

The converters with the specified transformers and resonant tank capacitances were built, measured and compared with the predictions of Table II. The obtained converter designs were implemented by modifying two custom power supplies. The original transformers and capacitors were replaced with the ones listed in Table IV. The original control IC has been replaced by external driver circuitry to drive the MOSFETs from a signal generator (see Figure 6). The external driver IC was selected to have comparable parameters, i.e. driving current and dead time, with the original controller, and the gate circuitry (diode-resistor networks) is left unchanged. Therefore, the switching behavior of the MOSFETs is not affected.

The converter now operates as an open-loop system with manually controlled output voltage. A digital voltmeter is used to measure the output voltage directly on the board via separate wires to eliminate the voltage drop over the resistances of the connectors and the connecting wires through which relatively high current (4.25 A) is flowing. The modification of the converter control is required because the tolerance of the control loop of the original supplies is observed to be $\pm 0.5\ V$. This tolerance is above the requested value of 0.5% (i.e. $\pm 0.12\ V$) [5].

The primary current is registered in the wire loop soldered over the PCB (see Figure 6) with a current probe and a digital oscilloscope, which is capable of calculating the RMS value of the signal. The temperatures are registered by painting the converter surface to have the same emissivity coefficient everywhere and measuring the surface temperatures with the IR camera inside the closed temperature chamber (see Figure 4).

As it can be seen from Table IV the discrepancy between the realized and targeted parameters is in the order of 10%...15%. However, it is difficult to predict beforehand the sensitivity of the converter to the parameters of the transformer and the capacitor. Therefore, the converters of designs #3 and #7 were simulated with the measured values as described in [7]. The targeted results (the points of the Pareto front of Figure 5), as simulated, and as realized are listed together in Table V.

In Table V the switching frequency at which the output voltage $U_0 = 23.5\ V$ is achieved, the core temperature ΔT_{core}, and the RMS value of the primary current $i_{Trpri}(RMS)$ are registered. The discrepancies

Table IV: Targeted and realized converter circuit parameters

Converter	Parameter	Notation	Targeted	Realized	Discrepancy, [%]
Design #3	Transformer				
	Primary inductance, $[\mu H]$	L_{p1}	675.0	663.0	1.8
	Primary DC resistance, $[m\Omega]$	R_{DCpri}	114.1	117.0	2.4
	Primary AC resistance, $[m\Omega]$	R_{ACpri}	208.6	194.0	7.5
	Secondary DC resistance, $[m\Omega]$ (*)	R_{DCsec}	12.7	15.0	15.3
	Secondary inductance, $[\mu H]$	$L_{p_{sec}}$	8.1	8.3	2.4
	Mutual inductance, $[\mu H]$	M	72.7	68.1	6.8
	Coupling coefficient	k	0.982	0.918	7.0
	Capacitors				
	Capacitance, $[nF]$	$C3+C4$	16.67	16.14	3.3
Design #7	Transformer				
	Primary inductance, $[\mu H]$	L_{p1}	1279.0	1335.0	7.0
	Primary DC resistance, $[m\Omega]$	R_{DCpri}	152.1	176.6	13.9
	Primary AC resistance, $[m\Omega]$	R_{ACpri}	203.9	241.3	15.5
	Secondary DC resistance, $[m\Omega]$ (*)	R_{DCsec}	12.7	15.0	15.3
	Secondary inductance, $[\mu H]$	$L_{p_{sec}}$	8.8	8.6	2.3
	Mutual inductance, $[\mu H]$	M	104.7	95.7	9.4
	Coupling coefficient	k	0.986	0.893	10.4
	Capacitors				
	Capacitance, $[nF]$	$C3+C4$	18.00	18.09	0.5

(*) The secondary AC resistance is very low and is difficult to measure therefore

between targeted and realized values, and between simulated and realized values are also shown. As it can be seen, the realized and simulated values (with the realized circuit parameters) match closely. For design #3 the largest discrepancy is 15.7% for the core temperature, and is 10% for the RMS of the primary current. However, the discrepancy between realized and targeted values is large (35.2% for the temperature of the core). The measurement errors of the *Tektronix TDS 340* digital oscilloscope which was used for the measurements is in the order of $\pm 5\%$ for the RMS value of the current and within $\pm 3\%$ for measuring the frequency [15]. This results in the variation of the measured value in the range $0.855\,A \ldots 0.945\,A$. The discrepancy of the temperature is explained by the fact that the primary current, and, consequently, the magnetizing current (because the output power is the same for all three values) is at least 1.21 and at most 1.34 times higher than the target. The higher magnetizing current creates $1.21 \ldots 1.34$ times higher flux density in the core. For the ferrite material the coefficients of GSE [12] are $x = 1.46$ and $y = 2.75$. For the case of sinusoidal excitation [2] the approximation of Steinmetz equation is

[2] In the case of LLC the current waveforms are almost sinusoidal [11]

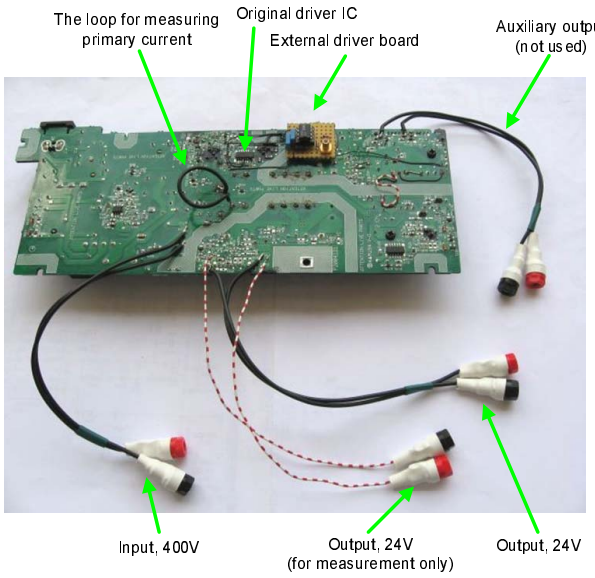

Figure 6: Modified converter board

$$P_v = c_m f^x B^y, \tag{5}$$

where P_v are losses per unit of volume and c_m denotes the material coefficient.

At the same time the switching frequency of the prototype is within $101.9\,kHz \ldots 108.2\,kHz$, or $0.78 \ldots 0.83$ of the targeted value. The core losses should be then at least $0.78^{1.46}\ 1.21^{2.75} = 1.17$, and at most $0.83^{1.46}\ 1.34^{2.75} = 1.68$ higher than the target. As a consequence, the forecasted temperature of the core should be also $1.17 \ldots 1.68$ times higher, because the thermal model is linear [5]. At the same time, the realized temperature is 1.54 times higher than the targeted one, which is within the range of $1.17 \ldots 1.68$. Therefore, the results for the design #3 are feasible.

The same conclusions are drawn for design #7. The predicted dissipated power in the core should be $1.38 \ldots 1.99$ times higher than the targeted one. Consequently, the temperature is expected to be $1.38 \ldots 1.99$ times higher as well. The measured value is only 1.55 times higher and is within the expected range of $1.38 \ldots 1.99$. Therefore the results for design #7 are feasible as well. At the same time, the simulated and the realized values of design #7 matched within 10%.

Considering that the simulated and the realized values show a good match, the large discrepancy between the realized and the targeted values is explained by the large sensitivity of the primary current to the values of the resonant tank capacitors and the transformer. If the transformer can be manufactured more precisely, the values of objective functions will match better.

Conclusions

A computer-aided approach for power converter synthesis was developed and verified by applying it to the LLC converter. The approach utilizes the custom accelerated simulator **M_SIM** [5]. Three design domains, namely electrical, thermal and magnetic are handled by this single synthesis tool. Multiple objectives and multiple tradeoffs are explored with the NSGA-II. The results of the optimization are presented in the form of Pareto fronts and were verified by means of brute-force simulation over the nodes of the grid in the variable space. NSGA-II approached the front quite closely but with about 9 times less simulation effort.

Each point of the Pareto front has its own optimal transformer design. The optimal transformers for two points of the Pareto front were built and measured. The resulting discrepancy between targeted and realized transformer parameters was within 15%. The converters with the measured parameters were simulated by **M_SIM**. The measurements showed a close match with the simulation. However, the targeted values of Figure 5a and Table II are different from the measured ones (see Table V). The discrepancy is explained by a high sensitivity of the resonant converter circuit to the transformer parameters. The approximate calculations showed that the results are feasible.

The developed tool, **M_SIM**, which makes use of the suggested approach is capable of handling any power converter topology and can be used for various power electronics optimization problems.

Table V: Targeted, realized and simulated values of the objective functions

Value	Switching frequency	Core temperature	RMS of the primary current
Design #3			
Targeted	130.6 kHz	18.6 K	0.704 A
Realized	105 kHz	28.7 K	0.900 A
Simulated	117.2 kHz	24.2 K	0.807 A
Discrepancy Targ.-Real.	24.7%	35.2%	21.5%
Discrepancy Simul.-Real.	11.9%	15.7%	10.0%
Design #7			
Targeted	51.8 kHz	28.6 K	0.678 A
Realized	50 kHz	44.2 K	0.840 A
Simulated	53.9 kHz	44.5 K	0.792 A
Discrepancy Targ.-Real.	4.9%	35.3%	19.3%
Discrepancy Simul.-Real.	9.1%	0.7%	5.8%

References

[1] K. Deb, A. Pratap, S. Agrawal, T. Meyarin: A Fast and Elitist Multiobjective Genetic Algorithm: NSGA-II, IEEE Transactions on Evolutionary Computation, vol. 6, no. 2, pp. 182-197, 2002

[2] D. E. Goldberg: Sizing Populations for Serial and Parallel Genetic Algorithms, Genetic Algorithms, IEEE Computer Society Press, IEEE Computer Society Press Technology Series, 1992

[3] J. G. Hayes, N. O'Donovan, M. G. Egan, T. O'Donnell: Inductance Characterization of High-Leakage Transformers, 2003 Applied Power Electronics Conference (APEC), vol. 2, pp. 1150-1156, 2003

[4] D. V. Malyna, J. L. Duarte, M. A. M. Hendrix, F. B. M. van Horck: A Comparison of Methods for Finding Steady-State Solution in Power Electronic Circuits, 4-th International Power Electronics and Motion Control Conference (IPEMC), vol. 3, pp. 1700-1705, August 2004

[5] D. V. Malyna, J. L. Duarte, M. A. M. Hendrix, F. B. M. van Horck: Power Converter Thermal Modeling Based on Experimental Parameter Identification, 2006 International Symposium on Industrial Electronics (ISIE), July 2006

[6] D. V. Malyna, J. L. Duarte, M. A. M. Hendrix, F. B. M. van Horck: Multi-Objective Optimization of Power Converters Using Genetic Algorithms, 2006 International Symposium on Power Electronics, Electrical Drives, Automation and Motion (SPEEDAM), pp. 713-717, May 2006

[7] D. V. Malyna, E. C. W. de Jong, J. A. Ferreira, M. A. M. Hendrix, J. L. Duarte, P. Bauer, A. J. A. Vandenput: Combined electrical and thermal modeling in power supplies, 2005 European Conference on Power Electronics and Applications (EPE), September 2005

[8] M. Sippola, R. E. Sepponen: Accurate Prediction of High-Frequency Power-Transformer Losses and Temperature Rise, IEEE Transactions on Power Electronics, vol. 17, no. 5, pp. 835-847, 2002

[9] E. Zitzler, K. Deb, L. Thiele, Comparison of Multiobjective Evolutionary Algorithms: Empirical Results, Evolutionary Computation Journal, vol. 8, no. 2, pp. 125-148, 2000

[10] K. Deb: Multi-Objective Optimization Using Evolutionary Algorithms, John Willey and Sons, 2002

[11] R. W. Erickson, D. Maksimovic: Fundamentals of Power Electronics, Kluwer Academic Publishers, 2001

[12] F. van Horck: A Treatise on Magnetics and Power Electronics, Eindhoven University of Technology, 2005

[13] E. Kreyszig: Advanced Engineering Mathematics, John Willey and Sons, 1999

[14] J.W. Nilsson: Electric Circuits, Addison-Wesley Publishing Company, 1990

[15] TDS 340, TDS 360 & TDS 380 Digital Real-Time Oscilloscopes. User Manual, Tektronix, Inc., ver. 070-9459-00